Journal of Structural Geology 32 (2010) 1125–1136

Contents lists available at ScienceDirect

Journal of Structural Geology

journal homepage: www.elsevier.com/locate/jsg

Magnetic fabrics as constraints on the kinematic history of a pre-tectonic granitoid intrusion, Kristineberg, northern Sweden

Pietari Skyttä [a,*], Tobias Hermansson [b], Sten-Åke Elming [a], Tobias Bauer [a]

[a] Division of Geosciences, Luleå University of Technology, SE-97187 Luleå, Sweden
[b] Boliden Mineral AB, SE-93681 Boliden, Sweden

ARTICLE INFO

Article history:
Received 4 February 2010
Received in revised form
24 June 2010
Accepted 29 June 2010
Available online 8 July 2010

Keywords:
Palaeoproterozoic
Skellefte district
Crustal evolution
Anisotropy of magnetic susceptibility (AMS)
VMS

ABSTRACT

Outcrop-scale correlations of deformation fabrics with low-field anisotropy of magnetic susceptibility (AMS) measurements revealed a two-stage structural evolution of the pre-tectonic, Palaeoproterozoic Viterliden intrusion in the Skellefte District, Sweden. The first deformation event reflected ~N–S compression during basin inversion, and comprised reverse dip-slip shearing along major ~E–W faults, whereas the low-strain lenses in between experienced penetrative deformation with a component of NE–SW elongation along the main foliation. This event is largely responsible for the present structural geometry regionally and locally, and also for the magnetic fabric of the rocks. In particular, the sub-vertical maximum principal susceptibility axes (K_{max}) within the high-strain zones are related to early dip-slip deformation, and were virtually unaffected by subsequent dextral strike-slip reactivation, which is recorded by sub-horizontal rock lineations. The strike-slip deformation reflects ~E–W bulk shortening and may regionally be correlated with reverse faulting along a ~N–S trending major shear zone east of the study area.

1. Introduction

The Kristineberg deposit is one of numerous volcanogenic massive sulphide (VMS) deposits in the Skellefte District (SD), Sweden (Fig. 1). The geometry of the Palaeoproterozoic crust within the SD is largely controlled by deformation along major fault zones, both during volcanism and sedimentation (Allen et al., 1996) and during the subsequent crustal shortening events (Bergman Weihed, 2001). However, the understanding of the geology is largely restricted to the area closely surrounding the deposits where intense ore-related alteration locally complicates the deformation pattern, just like in the Kristineberg area (Årebäck et al., 2005). Therefore, improved constraints about regional-scale deformation processes, including deformation kinematics, are needed to understand the structural evolution of the polydeformed area. Of particular interest are constraints about tectonic movements that affected the Kristineberg deposit (Fig. 2), where sub-horizontal tectonic flow is interpreted to be responsible for the transposition of the ore body into gently west-plunging orientation at depth (Skyttä et al., 2009). More generally, knowledge about structural control on the emplacement of ore deposits and their transposition during subsequent deformation is essential for targeting new deposits.

The Kristineberg deposit is hosted by felsic metavolcanic rocks that structurally overlie the composite, pre-tectonic Viterliden intrusion (1907 ± 13 Ma; Bergström et al., 1999), which is not largely affected by ore-related alteration, and appears structurally less complicated than the metavolcanic rocks. Measurements on the low-field anisotropy of magnetic susceptibility (AMS) of the Viterliden intrusive rocks, a widely used method to determine either magmatic fabrics in granitoids or solid-state fabrics in a variety of rock types (Kligfield et al., 1977; Goldstein, 1980; Rathore, 1980; Hrouda, 1982; Borradaile, 1988; Bouchez et al., 1990; Borradaile et al., 1992; Bouchez, 1997; Elming and Mattsson, 2001; Mattson and Elming, 2001; Pares and van der Pluijm, 2002, 2003; Evans et al., 2003), were therefore considered suitable for providing constraints about the regional crustal evolution.

It is generally agreed that the orientation of the minimum principal axis of magnetic susceptibility (K_{min}) is normal to the observed foliation plane (Khan, 1962; Hrouda, 1982; Borradaile, 1991), whereas correlating the orientations of the maximum principal susceptibility axes (K_{max}) with the rock fabric is not equally straightforward. In rocks with a weak pre-deformational fabric, K_{max} parallels the direction of the regional extension direction, whereas in rocks with a strong initial fabric it may parallel the initial, or the

* Corresponding author.
E-mail addresses: pietari.skytta@ltu.se (P. Skyttä), tobias.hermansson@boliden.com (T. Hermansson), sten-ake.elming@ltu.se (S.-Å. Elming), tobias.bauer@ltu.se (T. Bauer).

0191-8141/$ – see front matter © 2010 Elsevier Ltd. All rights reserved.
doi:10.1016/j.jsg.2010.06.020

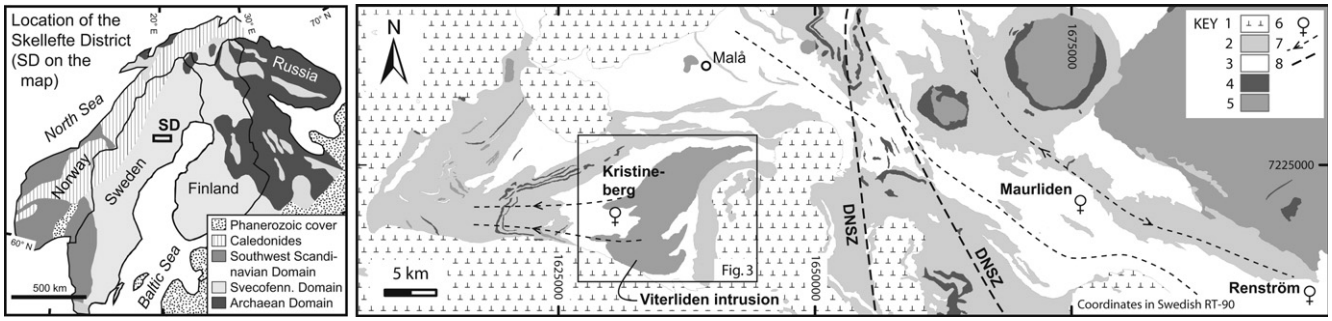

Fig. 1. Left: Geological overview of the Fennoscandian Shield. Right: Geological sketch of the western part of the Skellefte District. 1) Late- to post-tectonic granites, ~1.82–1.78 Ga. 2) Metasediments, ~1.87 Ga. 3) Skellefte Group metavolcanic rocks, ~1.89–1.88 Ga. 4) Mafic intrusions ~1.96–1.86 Ga. 5) Metagranitoids, ~1.90–1.88 Ga. 6) Active mines. 7) Axial trace of the main folds, plunge indicated by arrow. 8) Post-main deformation shear zones. DNSZ = Deppis-Näsliden Shear Zone (Bergman Weihed, 2001). Geology after the Geological Survey of Sweden.

regional extension direction, or be intermediate between these two (Borradaile and Tarling, 1981; Borradaile and Henry, 1997). The K_{max} orientation may also reflect the finite strain state of the rock. Although the magnetic fabric in low-grade sedimentary rocks is governed by dewatering and compaction-related layer-parallel shortening (Sagnotti and Speranza, 1993), K_{max} becomes parallel with the bedding/cleavage intersection with increasing strain (Hrouda and Janák, 1976), indicating interference between two

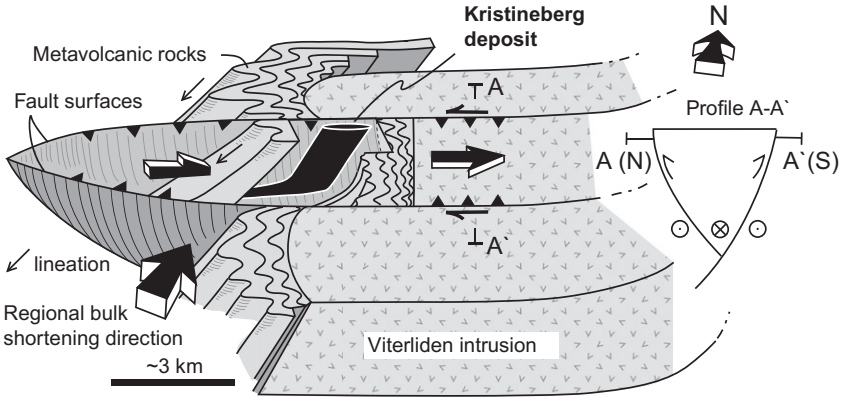

Fig. 2. A schematic block-drawing illustrating the geometric relationship between the Kristineberg ore deposit and the Viterliden intrusion, Skellefte Group metavolcanic rocks and the regional faults. Adapted from Skyttä et al. (2009).

Table 1
Petrological properties of the main lithological units within the Viterliden intrusion, including the mode of occurrence of magnetite grains in the studied AMS samples.

Location*	Rock type	Opaque minerals	Mt mode of occurence**						Mafic minerals	Amount of mafic minerals (%)	Style and/or intensity of tectonic fabric	Reference to fig.
			a	*b*	*c*	*d*	*e*	*f*				
I	Granite	mt, py, cpy, sph	x	(x)			x	x	bt, chl	~10	Moderate-intense, banded	Fig. 4c, h
II	Hbl-tonalite	mt, py, cpy, sph, hm	x	(x)	x				bt, hbl, chl, tita	~30	Intense, sheared (dip-slip)	Fig. 4g, k
III	Hbl-tonalite	mt, py, sph	x				x		bt, hbl	~30	Moderate	Fig. 4a, i
IV	Qtz-plg porphyritic tonalite	mt, py, sph	x[a]	x[b]			x			~10	Intense, sheared (strike-slip)	Fig. 4d
V	Hbl-tonalite	mt, py, hm	x	(x)		x			hbl, bt	25	Weak	Fig. 4j
VI	Hbl-tonalite	mt, py	x	x					hbl	15–20	Weak to moderate	
VII	Qtz-plg porphyritic tonalite	sph							chl	15	Intense	Figs. 4e and 7c (S-part)
	Hbl-tonalite	mt, sph	x	x					hbl, bt	15–20	Weak	Fig. 7c (N-part)
VIII	Chl-qtz-mylonite	mt, py, sph	x	x		(x)		(x)	chl	20	Intense, sheared (strike-slip)	Fig. 4f, l
IX	Hbl-tonalite	mt, py	**x**						bt, hbl, chl, epi	~20	Moderate	

* Roman numerals refer to AMS sites, shown in Fig. 3.
** Occurence of mt: (a) equant grains, (b) elongate grains, (c) aggregates of elongated grains, (d) aggregates with no specific preferred orientation, (e) lamellae along bt and chl basal cleavage planes, (f) inclusions along bt-cleavage planes.
mt = magnetite, py = pyrite, hm = hematite, cpy = chalcopyrite, sph = sphalerite, bt = biotite, ms = muscovite, chl = chlorite, hbl = hornblende, epi = epidote, tita = titanite, qtz = quartz, plg = plagioclase.
[a] Predominant in horizontal section.
[b] 50% of the mt in vertical section.

competing sub-fabrics (Borradaile and Tarling, 1981). With progressive deformation, K_{max} will be transposed into parallelism with the maximum principle strain axis (Borradaile and Henry, 1997). However, the orientation and magnitude of the finite strain do affect the distribution of the magnetic fabric elements, but so does the initial fabric pre-dating the observed deformation. Deviations of the K_{max} orientations from the rock lineations may be caused by partial overprinting of magnetic fabrics by subsequent deformation (Benn et al., 1993), the presence of intrafolial folds (Hrouda and Kahan, 1991), or complex mineralogy, such as due to oxides (Ruf et al., 1988) or silicates (Rochette et al., 1992).

The regional-scale focus of many of the publications about the magnetic fabric of deformed rocks (e.g. Hrouda and Janák, 1976; Mattson and Elming, 2001) may explain some of the reported variability between AMS and the rock fabric at the smaller scale, which necessitates the smaller scale investigation of this variability to ascertain its particular cause(s). Improvements in the understanding of the relation between K_{max} and rock lineations within complexly deformed regions are another goal of this manuscript. Given that the Viterliden intrusion is pre-tectonic with respect to regional deformation, we can study the style and degree of overprinting relations between different magnetic and rock fabric elements generated during separate deformation phases to gain insight into the variability.

AMS signature of samples taken from ten localities representing low- to high-strain structural domains within the Viterliden intrusion were measured and the results were related to sample mineralogy, outcrop-scale strain patterns, rock fabrics and inferred deformation kinematics in the field and in thin sections. In particular, orientation and orientation distribution of K_{min} and K_{max} were geometrically compared to rock foliations and lineations within a regional-scale geological framework. Measurements for the degree of magnetic anisotropy and the magnetic shape fabric were correlated with field observations to locally evaluate relationships among the finite strain, anisotropy degree and the style of deformation. Temperature variations of susceptibility were measured to constrain the mineral species that are the magnetic carriers of the samples.

In this paper, we show the advantage of combining magnetic fabrics and structural geology elements at the outcrop-scale to constrain the deformation history and kinematics of moderately to intensely deformed Precambrian terranes. The outcrop-scale

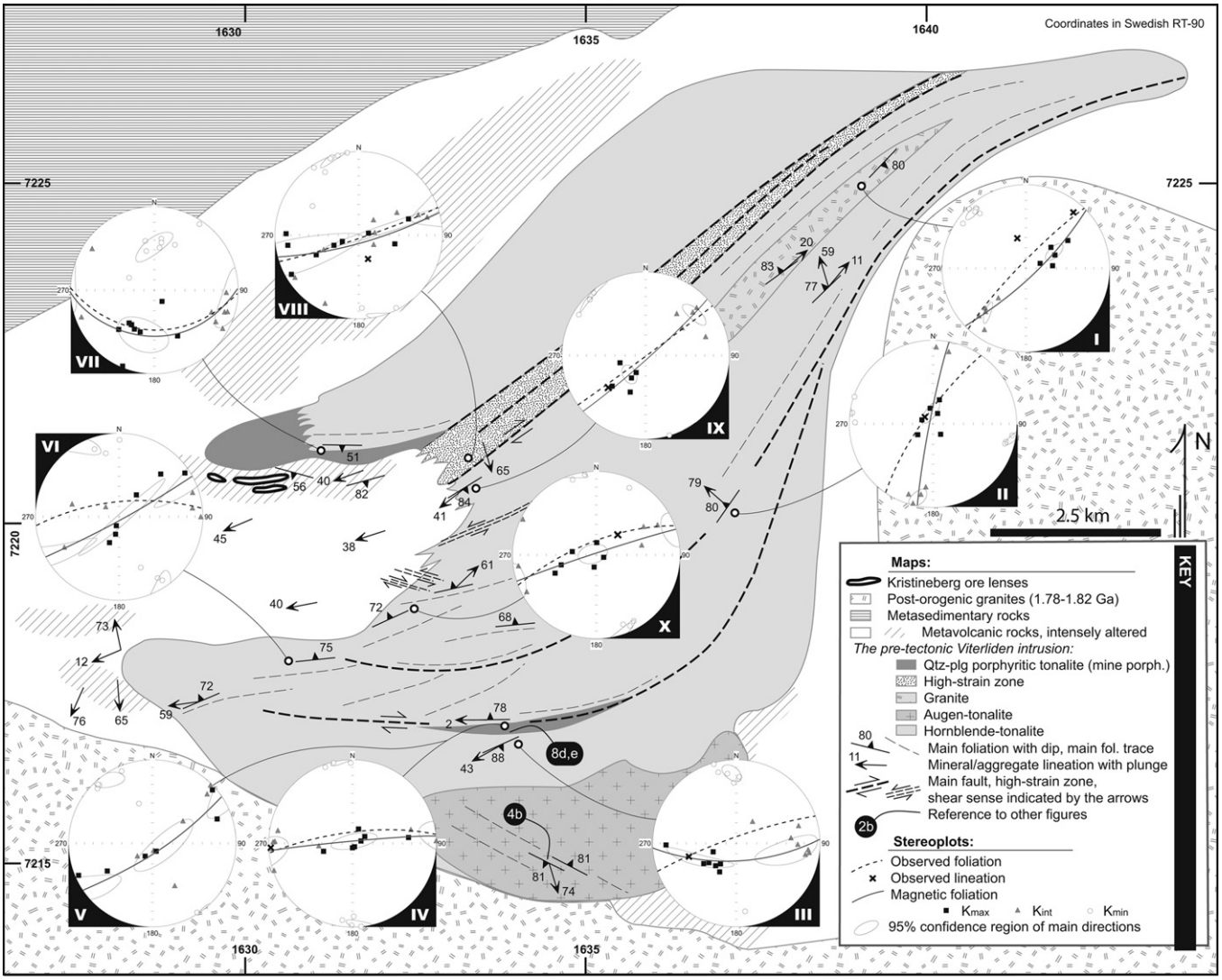

Fig. 3. Geological map of the Viterliden intrusion with lower-hemisphere, equal-area stereographic projections showing the orientations of the magnetic fabrics as defined by the AMS measurements. K_{max}, K_{int} and K_{min} correspond to the maximum, the intermediate and the minimum principal axis of magnetic susceptibility, respectively. References to localities with AMS measurements are given by Roman numerals. Lithostratigraphy modified after Galley and Bailes (1999).

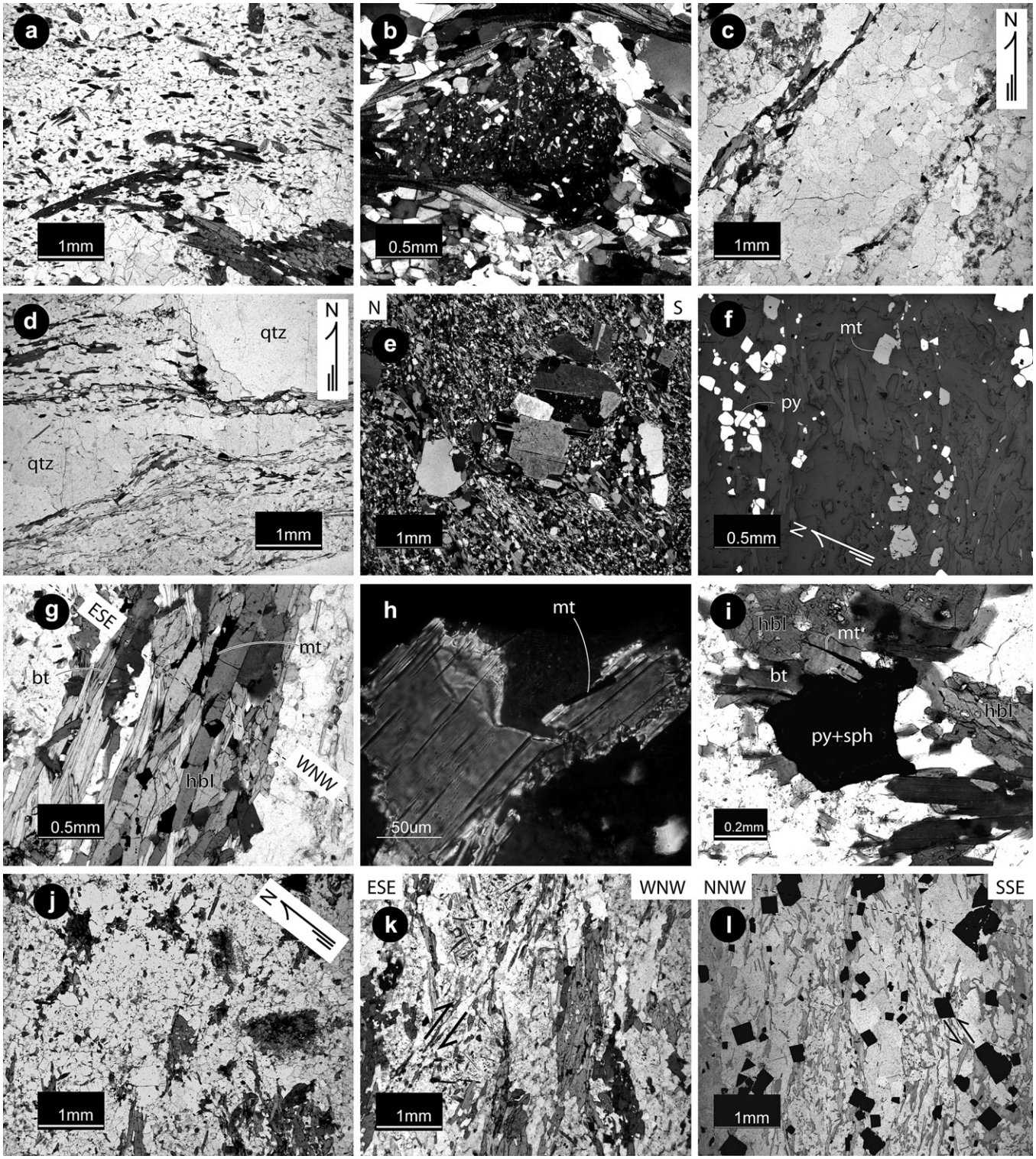

Fig. 4. Microphotographs of the main lithological units and microfabrics of the Viterliden intrusion. Sections are cut parallel with the mineral lineation. a) Intermediate-strain hornblende-tonalite showing aligned hornblende and biotite grains defining the main foliation, and end-sections of less aligned hornblende grains. Locality III, section dips WSW, view towards ENE (image rotated). b) Augen-structured biotite-tonalite. Section dips steeply E, view towards W (image rotated). c) Quartz-feldspar and mica-rich bands define the gneissic foliation of the granite. Locality I, horizontal section. d) Sheared quartz-plagioclase porphyritic tonalite showing dynamic high-T recrystallization and stretched quartz-ribbons with dextral asymmetries. Locality IV, horizontal section. e) Strong foliation in the mica-bearing quartz-plagioclase porphyritic tonalite north of the Kristineberg mine. Locality VII, vertical section, view towards E. f) Equant and weakly elongate pyrite and magnetite grains; magnetite grains are aligned along the mylonitic foliation trace. Locality VIII, horizontal section. g) Elongate magnetites defining a sub-vertical mineral lineation, in association with biotite and hornblende grains. Locality II, near-vertical section, view towards SSW, the dashed line indicates the horizontal level. h) An elongate magnetite grain enclosed in a biotite and having a sub-parallel orientation with the basal cleavage of the biotite grain. Locality I, horizontal section. i) Elongate magnetite grains inserting in between the biotite cleavage. Locality III, section dips WSW, view towards ENE (image rotated). j) Low-strain intrusive rock with poorly aligned hornblende and biotite grains. Locality V, horizontal section. k) A steeply ESE-dipping shear zone with reverse kinematics (dextral in the image) truncates the main foliation of a hornblende-tonalite. Locality II, near-vertical section, view towards SSW. l) Chlorite and opaque-rich, intensely sheared rock from the shear zone at locality VIII. Vertical section, view towards ENE, the dashed line indicates the horizontal level. See Table 1 for abbreviations.

control on the AMS analysis point locations is shown to be essential because much of the variation in the AMS signature arise from decimetre–metre scale lithological or structural variations. This approach also proved to be effective in distinguishing magnetic and rock fabric elements derived from separate deformation events. Orientation of the magnetic susceptibility axes within high-strain zones is shown to provide essential constraints about early deformation stages, which commonly are overprinted by subsequent events, such as fault reactivation in this case. In contrast to the high-strain zones, both the AMS signature and rock fabric of the lower-strain rocks are shown to have developed during one single deformation event.

2. Geological setting

The bedrock of the Skellefte District is composed of ~1.91–1.85 Ga Palaeoproterozoic Svecofennian supracrustal and associated intrusive rocks. The Viterliden intrusion (1907 ± 13 Ma; Bergström et al., 1999) belongs to the oldest suite of intrusions within the district. Its youngest phase, the "mine porphyry", is known to post-date the Kristineberg ore deposit (Årebäck et al., 2005). The intrusion occurs in the core of the regional west-plunging Kristineberg antiform (Fig. 1), and is overlain by the VMS-bearing Skellefte Group metavolcanic rocks and the Vargfors Group metasedimentary rocks, 1.89–1.88 Ga and ~1.87 Ga, respectively (Billström and Weihed, 1996). Late- to post-tectonic 1.82–1.78 Ga Transscandinavian Igneous Belt (TIB) granitoids bound the Kristineberg antiform to the west and south. The massive sulphide deposits within the Skellefte District occur predominantly along the top of the dominantly felsic Skellefte Group volcanic complex, itself attributed to a stage of extensional continental margin arc volcanism (Allen et al., 1996). The pre-TIB rocks were deformed and metamorphosed during the Svecokarelian Orogeny at 1.90–1.80 Ga (Weihed et al., 2002), under pressures below 330 MPa and peak temperatures at ~600 °C (Kathol and Weihed, 2005).

Structural geometry of the Skellefte District results from basin inversion due to an early extension overprinted by a subsequent

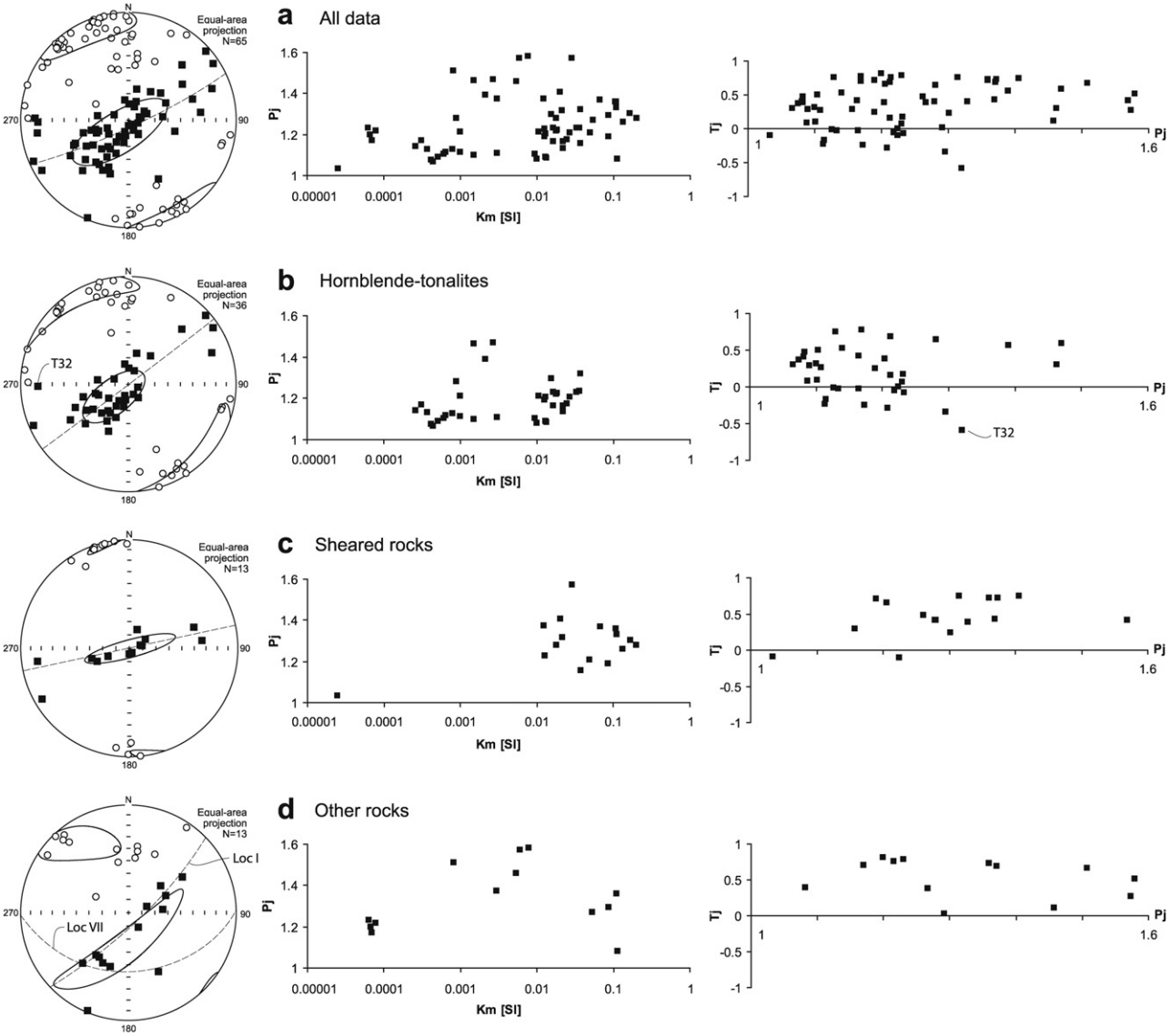

Fig. 5. Summary of the AMS results. Dashed lines indicate the magnetic foliation (S_{mag}), other symbols in stereoplots as in Fig. 3. a) All samples; S_{mag} 155/84, b) hornblende-tonalites; localities II, III, V, VI, IX, X; S_{mag} 143/89; sample T32 indicated separately, c) sheared rocks; localities IV, VIII; S_{mag} 168/90, d) other rocks; localities I and VII; S_{mag} 136/81 and 179/44, respectively. 95% confidence ellipses are plotted (Jelinek, 1978). Stereographic projections are lower-hemisphere, equal-area.

compression, the greatest strains being localized into reactivated normal faults and their vicinity (Allen et al., 1996; Bauer et al., 2009). This succession of events leads to structural complexity and large strain variations both across and along the regional Kristineberg antiformal structure (Malehmir et al., 2007; Skyttä et al., 2009). The main deformation is dated between ~1.875 Ga and ~1.80 Ga (Kathol and Weihed, 2005) and the peak of metamorphism around ~1.85–1.80 Ga (Weihed et al., 1992; Billström and Weihed, 1996). Although regional evidence exists for a localized overprint along major ~N–S trending shear zones at ~1.80 Ga (Bergman Weihed, 2001; Weihed et al., 2002), no such cross-cutting high-strain zones have been recognized in the Kristineberg area.

3. Lithology, deformation structures and microstructures

The main rock type of the Viterliden intrusion is a hornblende-tonalite (Fig. 4a,j; Table 1). The other lithologies include augen-structured, gneissic biotite-tonalite (Fig. 4b), granite (Fig. 4c) and quartz-plagioclase porphyritic tonalite (Fig. 4d,e). The contacts between the intrusive phases and the intrusive and volcanic rocks are generally sheared, thus making it impossible to determine the relative ages between units. The sheared rocks are mostly characterized by an increased amount of micas, similar to the quartz-plagioclase porphyritic tonalite within the alteration halo of the Kristineberg ore deposit (Fig. 4e; southern part of Locality VII: Figs. 3 and 7c). The latter unit is referred to as the "mine porphyry" by Årebäck et al. (2005). Opaque minerals in the intrusive rocks include pyrite, magnetite, hematite and translucent sphene. Magnetite occurs as equant to elongated grains, and less frequently as aggregates often associated with the mafic rock-forming minerals (Fig. 4g; Table 1). In some samples, magnetite occurs along the basal cleavage planes of biotite either as inclusions or inserting in between (Fig. 4h and i, respectively). Hematite occurs as a secondary mineral replacing pyrite at grain boundaries, or as an alteration product of magnetite.

Strain was partitioned into a few sub-vertical, curviplanar shear zones with low-strain tectonic lenses in between. The former display intense mylonitic fabrics (Fig. 4d,l), whereas weak to moderate foliations (Fig. 4a,j) characterize the latter. The main foliation roughly parallels the shear zones, strikes ~NE–SW in the north and curves into a nearly east–west trend in the south. It is steeply-dipping to sub-vertical and locally shows alternating dip directions. In the low-strain lenses, its strike is slightly oblique to that of the high-strain zones. The foliation is penetrative and mostly defined by alignment of mica grains, whereas the hornblende grains occur both as elongated grains sub-parallel with mica, and as more equant grains or aggregates showing no distinct preferred orientation (Fig. 4a), giving the rocks an SL-shape fabric. However, within the high-strain zones, but also locally within the tectonic lenses, the rocks are dominantly LS- to L-tectonites (e.g. at Locality III; Fig. 3).

Mineral lineation is defined by the zonal orientation of mica and the alignment of hornblende. In high-strain zones, it plunges either down-dip when associated with reverse dip-slip kinematics, or sub-horizontally when associated with dextral strike-slip kinematics (Fig. 4k and d, respectively). Along the western margin of the intrusion (Fig. 3; between AMS localities IX and X), small-scale shear zones with both sinistral and dextral shear senses are observed. The larger shear zones (Fig. 3; localities IV and VIII) express dominant dextral strike-slip and reverse dip-slip components (Figs. 7d and 4l, respectively). Outside the shear zones, the lineation dominantly plunges moderately towards SW, except to the south of locality I (Fig. 3) where both steeply plunging and sub-horizontal lineations are observed close together.

4. AMS investigations

4.1. Sampling and laboratory techniques

A total of 65 samples were collected from ten sites of the Viterliden intrusion using a portable drill or as hand specimens. The samples were oriented with magnetic and sun compasses. The AMS and the temperature variation of the magnetic susceptibility were measured using Kappabridge KLY-3 and CS-3 instruments, respectively (Geofyzika Brno).

4.2. AMS results – general

The bulk magnetic susceptibility (K) of the lithological units varies between 2.51×10^{-05} SI and 2.02×10^{-01} SI with a predominance in the lower end of the range. The degree of anisotropy (Pj; Jelinek, 1981) displays values up to 1.58 (Fig. 5a). Except for a few outliers, the hornblende-tonalities exhibit weakly increasing anisotropy with increasing susceptibility (Fig. 5b). Other lithological groups do not show any clear correlation between Pj and K (Fig. 5c,d).

The shape of the magnetic anisotropy ellipsoid is defined by the shape parameter Tj (Jelinek, 1981), for which $-1 < Tj < 0$ characterizes prolate ellipsoids, $0 < Tj < 1$ oblate ellipsoids, and $Tj = 0$ neutral ellipsoids, correlating with the usual constrictional, flattening and plane-strain deformation regimes of structural geology, respectively. The majority of the Kristineberg samples plot as oblate ellipsoids, and those plotting as prolate ellipsoids are mostly

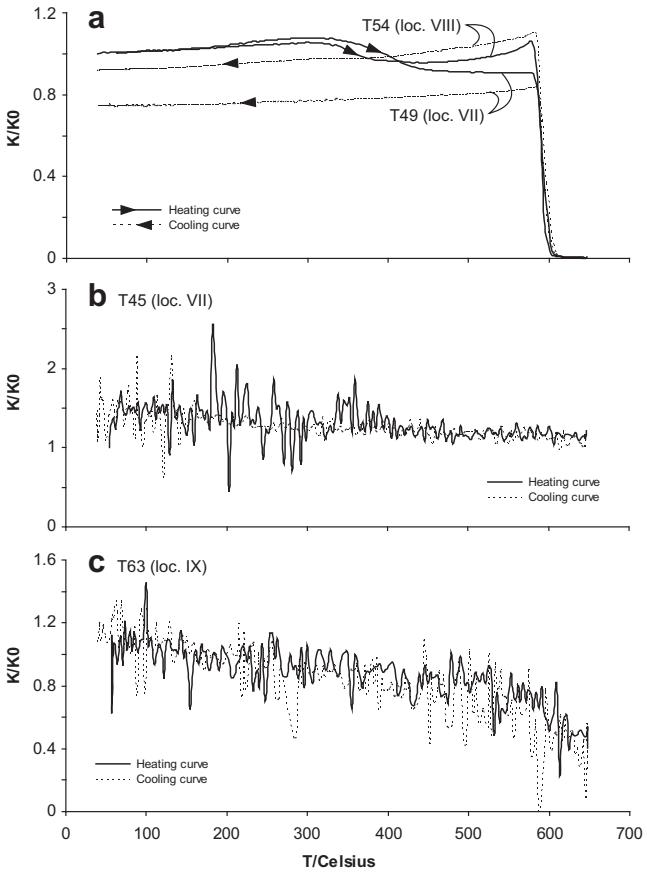

Fig. 6. Magnetic susceptibility versus T of selected rocks, indicative a) magnetite, and b) and c) paramagnetic minerals, as the carriers of the rock susceptibility.

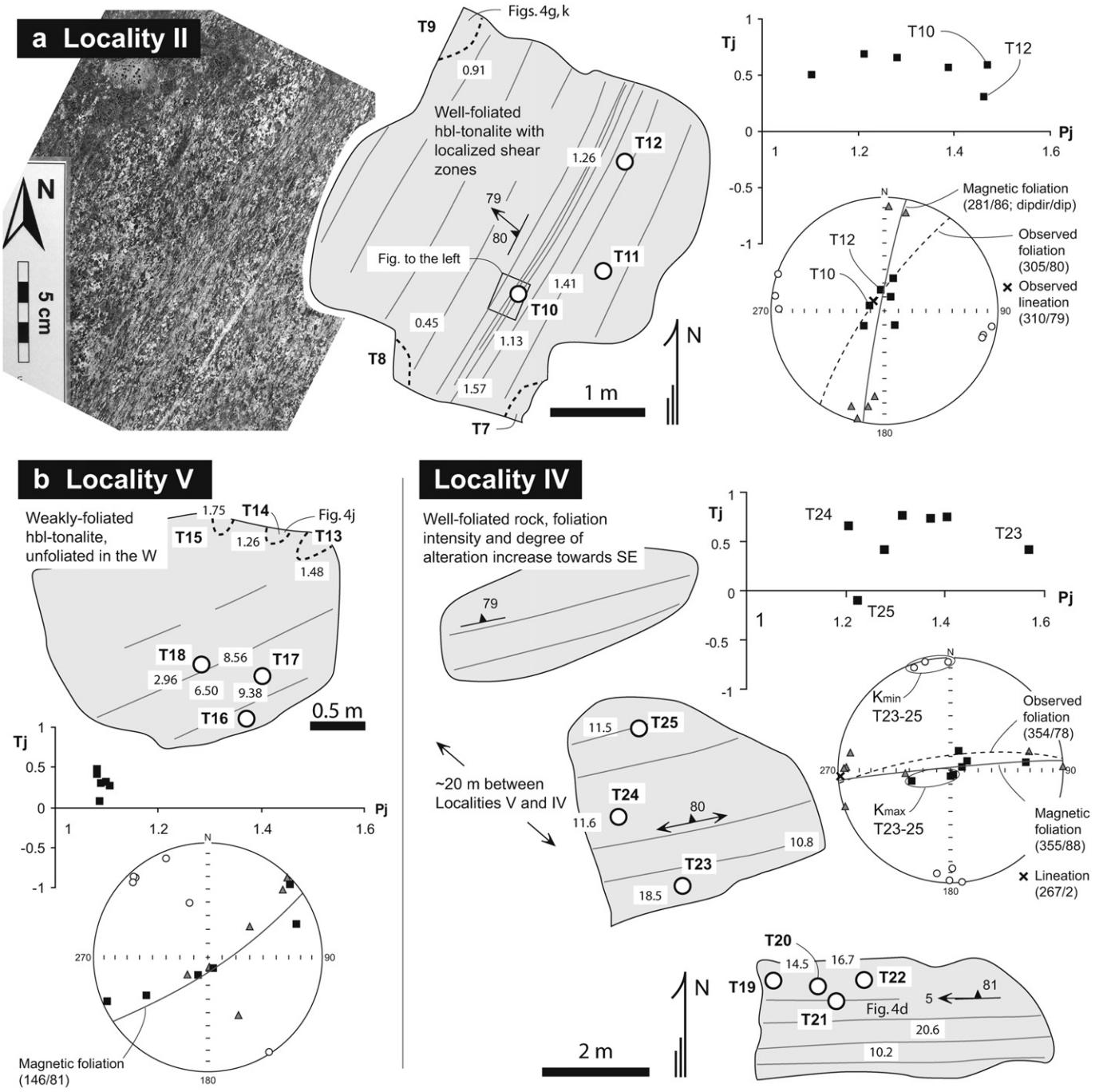

Fig. 7. Correlating the magnitude and orientation of the magnetic fabrics with outcrop-scale strain patterns. Outcrop sketches, anisotropy shape factor (*Tj*) versus degree of anisotropy (*Pj*) diagrams, and stereoplots with magnetic and rock fabric element orientations are provided for all the localities. Symbols for AMS plots as in Fig. 3. a) Locality II: (left) Narrow discrete shear zone transects a weakly to moderately-foliated hornblende-tonalite with variably flattened mafic magmatic enclaves (not present in the photo). b) Locality V (left): The cluster of K_{min} axes of AMS defines a clear magnetic foliation of a low-strain hornblende-tonalite although no clear tectonic foliation was present when observed in the field. Locality IV (right): The samples T23-25 cluster rather well in orientations despite the large differences in the magnitude and style of magnetic anisotropy. c) Locality VII: The well-foliated, low susceptibility rock defines a rather tight cluster of K_{max} axes, while the high-susceptibility rock in the north shows a more scattered AMS pattern. d) Locality VIII: K_{max} orientations of the sampled mylonites spread along the mylonitic foliation surface (left), whereas the three sampled granitoid boudin fragments show a considerable variation in both their K_{max} and K_{min} orientations (right).

hornblende-tonalites (Fig. 5b). The mylonites plot as oblate ellipsoids except for two samples that are prolate but nearly neutral (Fig. 5c).

The K_{min} axes form a modal concentration coincident with the poles of the foliation, which is reflecting steeply-dipping to sub-vertical foliations striking ~SW–NE, except in the case of K_{min} poles related to the high-strain shear zones that are mainly E–W striking (Figs. 3 and 5c).

Although rather scattered when considered all together, the K_{max} axes for the hornblende-tonalites lie on a steeply-dipping great circle trending NE–SW and show a predominant steep to moderate plunge towards the SW (Fig. 5b). The K_{max} axes in the high-strain zones vary significantly in attitude along the steeply-dipping, ENE–WSW trending magnetic foliation, however displaying a sub-vertical mean within-site plunge (Fig. 5c). K_{max} data from the other rocks scatter either along sub-vertical, NE–SW

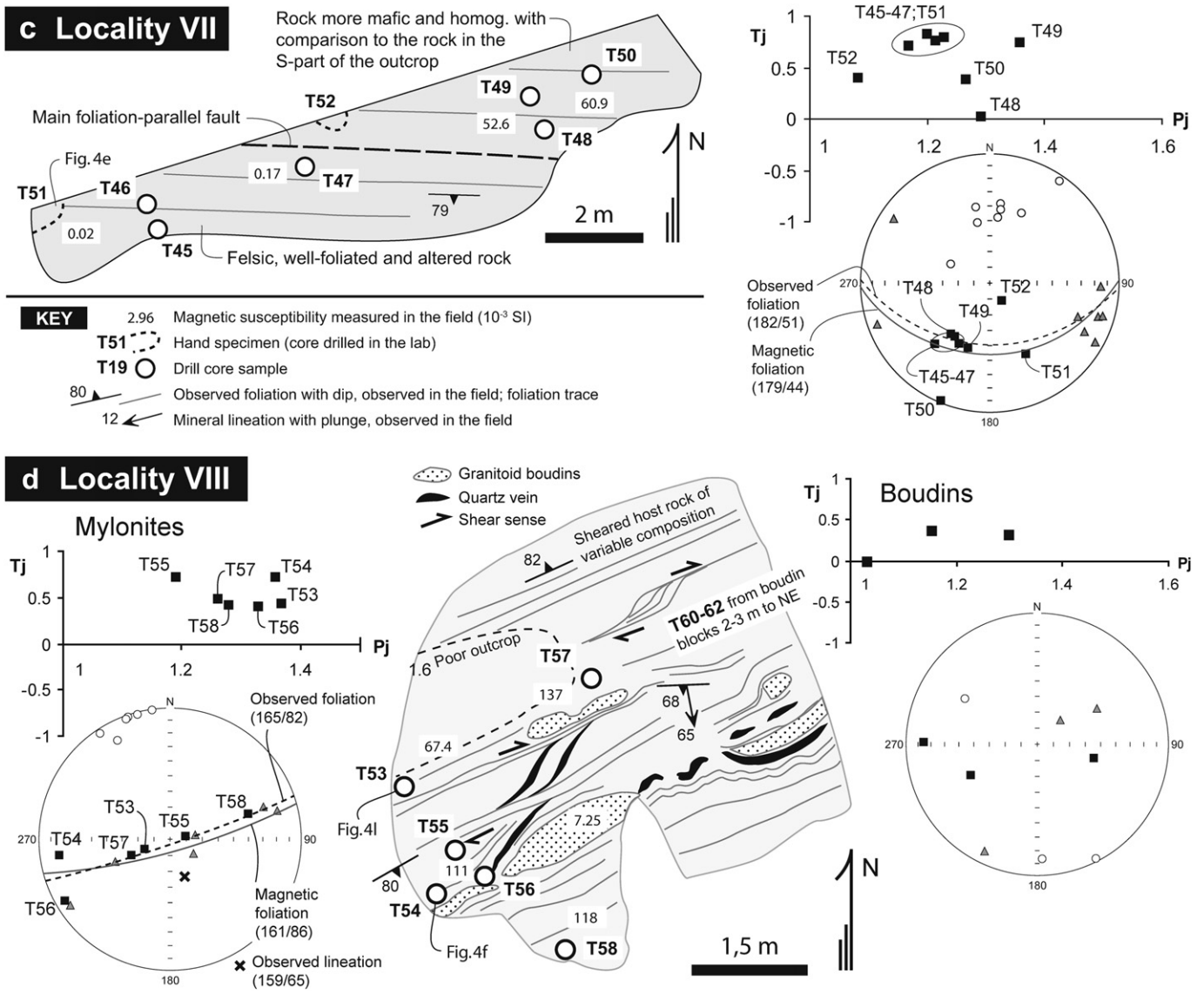

Fig. 7. (*continued*)

trending, or south-dipping, E–W trending magnetic foliation surfaces (Fig. 5d; locs. I and VII).

The characteristic abrupt decrease of the magnetic susceptibility at temperatures ~583 °C for the most samples suggest that magnetite is the main carrier of magnetic susceptibility (Fig. 6a; Hrouda et al., 1997). However, in two of the eight measured samples (Fig. 6b,c) the characteristic gradual decrease in a zig-zag pattern of the susceptibility as a function of temperature infer that paramagnetic minerals, mainly biotite, hornblende and chlorite, generate the magnetic signature.

4.3. Correlations between geological observations and magnetic fabrics

The orientation of magnetic foliation generally coincides well with the rock foliation (Fig. 3). Also the strength of foliation ranging from weak (Fig. 4j) to moderate (Fig. 4a) to strong (Fig. 4c,d), as defined by the degree of alignment of the rock-forming minerals, correlates with the strength of the clustering of the K_{min} axes. This correlation is attested by the comparison between localities IV + VIII, which are strongly deformed and have well-defined magnetic foliations, and locality V in which the less-pronounced clustering of K_{min} reflects the low-strain state of the rock (Figs. 3 and 4j). Also the degree of anisotropy locally correlates with the deformation fabric intensity at the outcrop-scale. K_{max} axes and the rock lineation for most of the hornblende-tonalites are sub-parallel, whereas other rock types show larger angular variations between the two.

Magnetic foliations deviate significantly from their tectonic counterparts at locations II, III, and VI. At locality II, the magnetic foliation strikes more N–S compared to the observed SSW–NNE striking foliation (Fig. 7a), which is interpreted as reflecting a ~N–S striking pre-shear fabric influencing the magnetic measurements. The degree of anisotropy correlates with the strain pattern across the outcrop, since the greatest values are recorded for the specimens in, or in the immediate vicinity of discrete shear zones (T10, 12). The subsequent development of more local, semi-brittle, ESE-dipping minor shear zones (Fig. 4k) has no influence on the magnetic data. At locality III, the magnetic and the observed foliations have similar strikes but opposite dip directions (Fig. 3). Intersection of these foliations corresponds to both the clustering of K_{max} axes and the lineation measured in the field. It is reasonable to infer that a foliation generated during a single deformation event

may vary considerably in orientation as long as it contains the tectonic lineation, in particular within rocks with L-tectonic affinities. Sample T32 further supports localized sub-horizontal, constrictional flow, as it has the highest *Pj*-value, gentler K_{max} than the other specimens at the site, and clearly plots in the prolate field (Fig. 5b). At locality VI, the deviation between the magnetic fabric and tectonic fabric is attributed to poor control on the latter due to bad outcrop condition.

The K_{max} orientations deviate from the rock lineations at localities I, IV, VIII and X. Furthermore, two lithological units with different K_{max} orientations were recognized at locality VII. At locality I, two rock lineations were observed: one sub-horizontal with a NE trend and another with steep NW-plunge, the latter coinciding with the K_{max} orientation (Fig. 3). The steep lineations are attributed to dip-slip, and the gentle ones to strike-slip deformation. At locality IV, the rock lineation is sub-horizontal, whereas the K_{max} axes define a sub-vertical site mean orientation (Fig. 7b). This indicates that the strike-slip movement, as observed in the field, may not have affected the magnetic carriers. Deflection of the regional magnetic foliation, as defined with AMS (loc. V) into the high-strain zone (loc. IV) is interpreted to result from local strike-slip deformation post-dating regional deformation. At locality VIII, the rock lineation shows a sub-vertical plunge, whereas the K_{max} orientations of the mylonitic layers, and the boudin blocks in particular, scatter in the magnetic foliation (Fig. 7d). The latter may be attributed to unevenly distributed strain and rotation of the boudins during shearing, whereas scatter in the K_{max} orientations of the mylonitic layers is inferred to result from a combination of the inhomogeneous shearing and the incomplete overprint of the older fabric. At locality X, the site mean of K_{max} axes is sub-vertical, and the observed lineation plunges steeply towards NE on the tectonic foliation surface (Fig. 3). However, no clear explanation for the deviation may be provided in this case. At locality VII, the AMS signature of the felsic, low susceptibility unit in the southern part of the outcrop is controlled by paramagnetic minerals, and its K_{max} orientations align well with the regional, SW-plunging mineral lineation (Figs. 3, 6 and 7c). By contrast, magnetite grains with a weak preference to parallelism with the weak tectonic foliation observed in the more mafic, high-susceptibility unit control the AMS signature in the northern part of the outcrop. Better K_{max} clustering is attributed to preferential strain localization into the felsic unit during compressional deformation.

These results clearly show that the presented magnetic fabrics may be correlated to tectonic deformation, and may therefore, together with the rock fabrics, be used as constraints for interpreting deformation kinematics and crustal evolution in the area. Furthermore, we infer that the strong coupling between the magnetic and tectonic fabrics implies that all of the recorded magnetic fabric elements reflect tectonic rather than magmatic features.

4.4. Horizontal versus sub-vertical fabric elements

Localities I, II and IV have steeply plunging K_{max} axes, whereas the rock lineations vary and are not concentrated sub-vertically (Fig. 8). Considering characteristics of the magnetic fabric, bulk susceptibility is greater at locality IV, but the anisotropy and AMS ellipsoid shape factor are similar between the three locations. Therefore, we interpret the magnetic fabric at the three locations to record the same deformation. Consequently, we interpret the variation in the rock fabric to reflect this fabric recording the effects of different deformation histories at the three localities. Specifically, the sub-vertical rock lineation and the parallel K_{max}

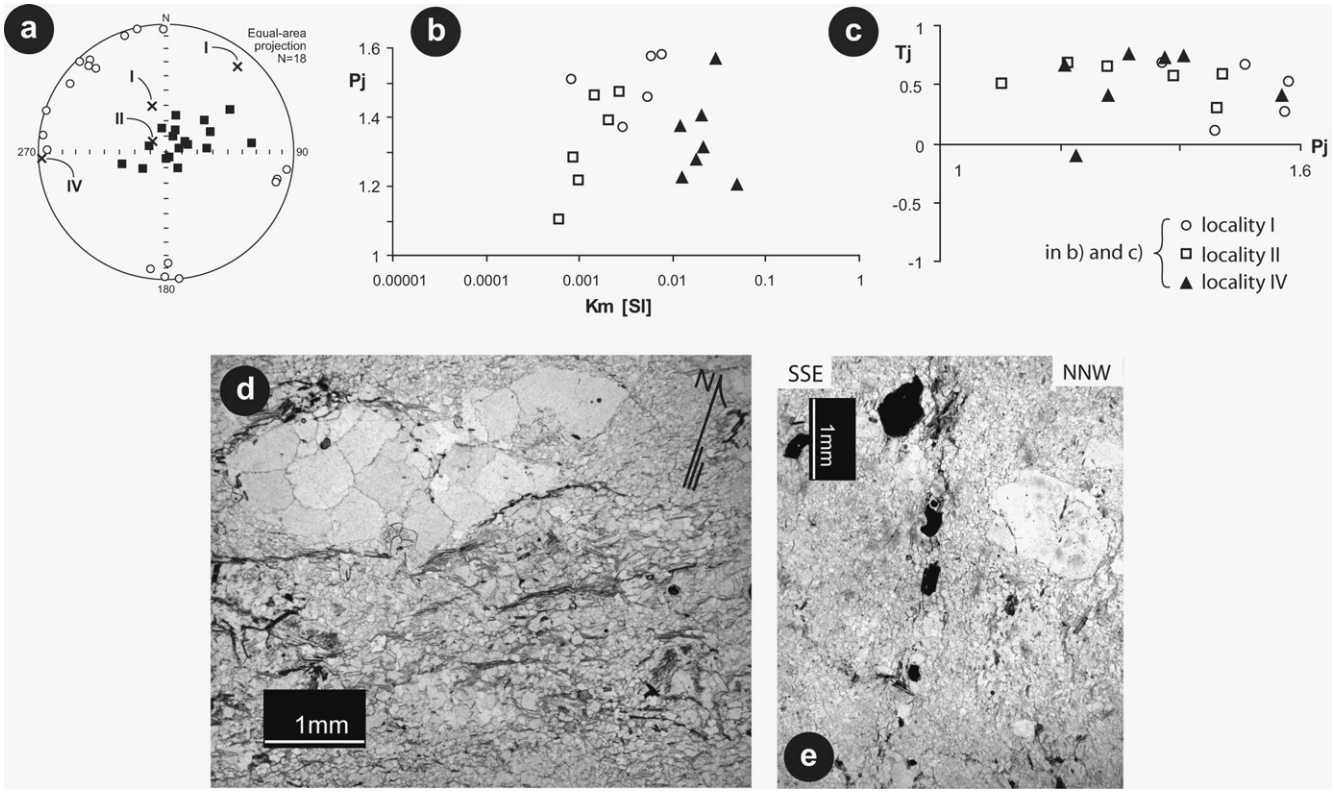

Fig. 8. Comparison of the AMS results of localities I, II and IV with elements of the rock fabric. a) Compilation of K_{max} and K_{min} axes (symbols as in Fig. 3) and rock lineations (crosses with associated locality numbers). b) Anisotropy degree vs. bulk susceptibility c) Magnetic shape factor vs. anisotropy degree. d) Horizontal section, parallel to the lineation, of a quartz-plagioclase porphyritic tonalite (compare with Fig. 4d) showing a clear solid-state foliation. e) Sub-vertical section, perpendicular to the lineation, of the same rock showing the weak foliation defined by the weak alignment of micas, and the large quartz-phenocrysts. The opaque minerals define a clear sub-vertical lineation that corresponds to the measured K_{max}.

site mean orientation at locality II (Figs. 3 and 7a) are attributed to reverse dip-slip shearing along a NE–SW trending high-strain zone. Analogously, the steep K_{max} orientations at localities I and IV, and the steep rock lineation at locality I (Figs. 3 and 7b), are correlated to the dip-slip deformation, whereas the horizontal tectonic lineations are related to a strike-slip overprint. Microstuctures clearly record the strong strike-slip overprint (Fig. 8d), whereas the shape and alignment of the magnetite/opaque minerals, responsible for the K_{max} orientations, were preserved, as shown by their dominantly equant and elongate shapes in sections parallel and perpendicular to the rock lineations, respectively (Fig.8e; Table 1).

5. Discussion

5.1. Magnetic and tectonic fabrics – constraints on the regional crustal evolution

Regional structural evolution within the Skellefte District is characterized by inversion tectonics, where initially extensional normal faults became reactivated with reverse kinematics during ~N–S compression (Fig. 9a; Allen et al., 1996; Bauer et al., 2009). Subsequently, a younger phase of E–W shortening caused reverse faulting along ~N–S trending large-scale shear zones (Fig. 9c; Bergman Weihed, 2001). In the Kristineberg area, the overprinting nature of the sub-horizontal rock lineations, associated with dextral kinematics along major high-strain zones, allows us tentatively correlate the dextral shearing with the regional E–W shortening event. Consequently, rock foliations and the associated steeply plunging rock lineations along high-strain zones, and the gently to moderate-plunging rock lineations in the low-strain tectonic lenses, are interpreted to result from the early ~N–S shortening event. The sub-vertical rock lineations may actually be directly linked to reverse dip-slip shearing (Fig. 4l), and the parallel K_{max} orientations in the high-strain rocks further indicate the importance of the early dip-slip event as responsible for the formation of the rock and magnetic fabrics, and eventually, the geometry of the crust in the area. The high-strain zones display oblate magnetic ellipsoids (Fig. 5c), which we infer to indicate that early reverse faulting took place under flattening conditions.

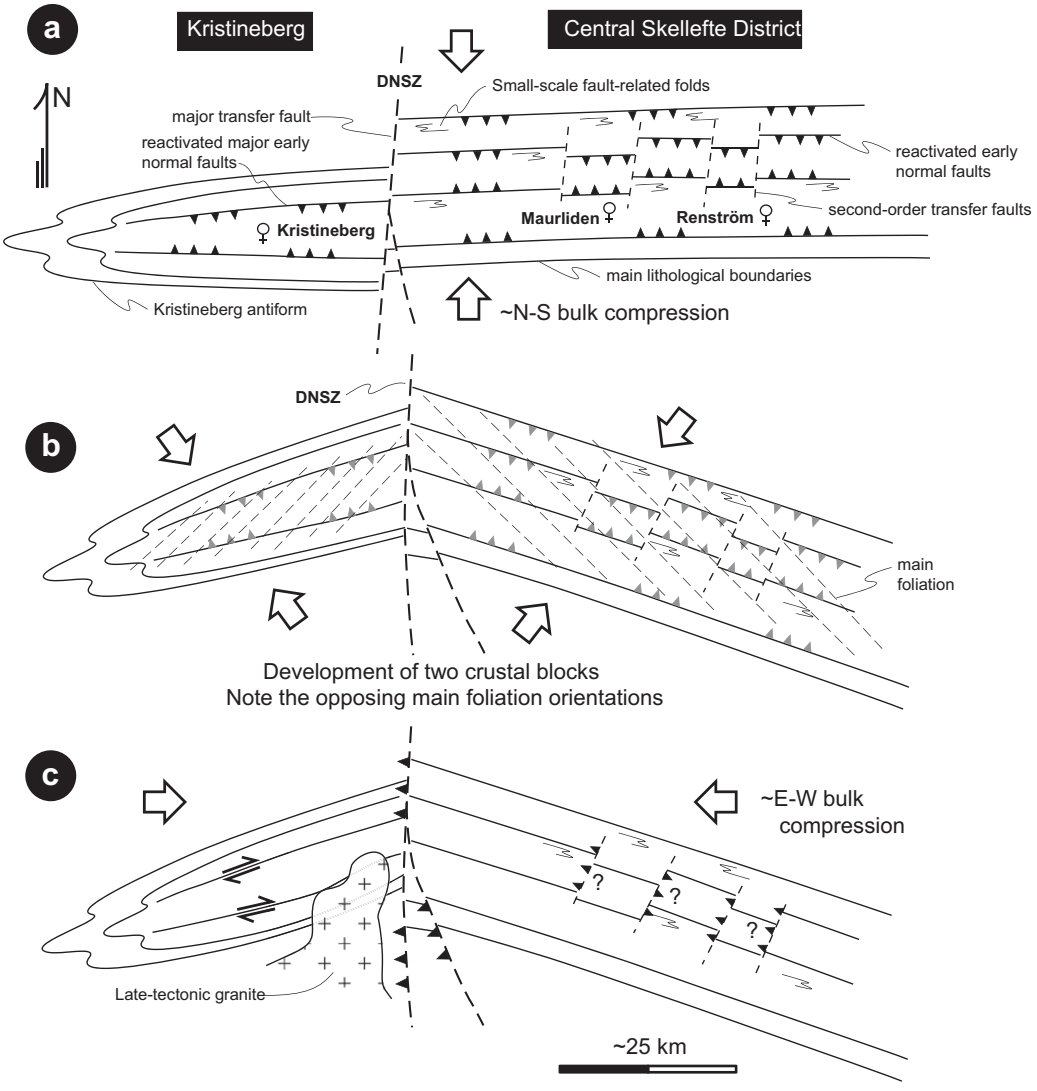

Fig. 9. A schematic model of the structural evolution in the Kristineberg and Central Skellefte District (CSD) areas. a) Inversion of early normal faults with reverse kinematics and down-dip lineations during ~N–S compression. b) Progressive N–S compression and concurrent activity along the Deppis-Näsliden Shear Zone (DNSZ; Bergman Weihed, 2001) led to different bulk shortening directions between the Kristineberg and the CSD areas. The main foliation was developed either during this stage, or coevally with the normal fault reactivation. c) The youngest deformation event was separate from the previous ones. It was characterized by ~E–W shortening and formation of strike-slip zones in the Kristineberg area, reverse dip-slip deformation along DNSZ, and possibly along the transverse faults in the CSD area.

The oblique orientation of the tectonic foliation in the low-strain lenses either is due to counterclockwise rotation of the bulk compression during progressive crustal shortening that followed fault inversion (Fig. 9b), or due to strain partitioning between the major faults and the tectonic lenses. The gently to moderately SW-plunging rock lineations frequently observed in the Viterliden intrusion may be correlated with those in the metavolcanic rocks in the vicinity of the Kristineberg deposit, and are considered to reflect a component of NE–SW elongation along the main foliation surfaces during the ~N–S bulk shortening. The sub-horizontally SW-plunging K_{max} axes and prolate AMS ellipsoids in the low-strain lenses are attributed to localized sub-horizontal, constrictional flow within a regional deformation regime characterized by flattening (Fig. 5a).

Dextral strike-slip overprint of the early ~N–S compression-related fabrics is typical along the ~E–W to NE–SW trending parts of main high-strain zones, whereas the overprint along the slightly more NNE–SSW trending parts of the high-strain zones in the core of the intrusion is characterized by more brittle faults with reverse kinematics (loc. II; Fig. 4k). This pattern of strain partitioning and kinematics during the overprinting deformation is compatible with a separate, post dip-slip structural event with ~E–W bulk shortening, hence corroborating the previous interpretations from the central parts of the Skellefte District (Bergman Weihed, 2001). This later deformation did not modify the magnetic signature of the rocks, except for at locality VIII, where intense strike-slip shearing is considered at least partly to explain the larger scatter of the K_{max} axes with respect to other localities along the high-strain zones. However, while no direct constraints on the finite strain at the locality are available, the shear-band and boudinage formation is attributed to strike-slip deformation.

The opposite vergence of the main foliation with respect to the main faults in the Kristineberg area and the central Skellefte District (Fig. 9b; Bauer et al., 2009) is inferred to mean that the Deppis-Näsliden shear zone (DNSZ) was already active during, or immediately after the first stage of the N–S compression, consequently most likely having its origin as a large-scale transfer fault generated during crustal extension. The early tectonic movements along the DNSZ at the onset of the basin inversion would have caused large-scale block-rotations within the Skellefte District that continued during the ~E–W compression event, possibly assisted by the emplacement of the late granites at ~1.80 Ga (Fig. 9c).

5.2. The role of sub-horizontal tectonic flow in shaping the Kristineberg ore body

The present study implies that the role of sub-horizontal tectonic flow in the Kristineberg mine (Fig. 2; Skyttä et al., 2009) was less important than previously suggested, as the early dip-slip event is shown to have had the most significant control on the structural geometry of the area, both in the mine and at the regional-scale. This interpretation is also in line with the dominant S-block-up reverse faulting in the Kristineberg mine (Fig. 4 in Årebäck et al., 2005), which led to folding and stacking of the deeper-seated ore lenses, and hence causing their transposition into gentler plunges at depth. Even though the sub-horizontal constriction during the early dip-slip event was of local extent, it may have been enhanced by localization into hinges of the reverse fault-related folds. The subsequent overprint during ~E–W compression was localized into the steeply-dipping, high-strain zones with strike-slip shear, and therefore did not cause penetrative transposition of existing structures across the region.

The role of the early dip-slip zones in the regional crustal evolution is emphasized even more as we infer that the quartz-plagioclase porphyritic tonalities were emplaced along them. Consequently, these major high-strain zones acted both as magma pathways during the emplacement of the intrusion, and as zones of deformation localization during the subsequent tectonic overprint.

6. Conclusion

1) The sub-vertical rock lineations and maximum principal anisotropy axes along high-strain zones transecting the Viterliden intrusion correlate with dip-slip deformation along reverse faults during ~N–S crustal shortening related to the regional inversion of pre-existing normal faults.
2) The rock and magnetic fabrics in the low-strain lenses between the high-strain zones are inferred to contain a component of NE–SW elongation developed during the dip-slip event.
3) The dip-slip event was largely responsible for the present structural geometry regionally and locally, and also for the magnetic fabric of the rocks.
4) Subsequent strike-slip shearing during ~E–W compression post-dated the dip-slip event, heterogeneously modified the tectonic fabric in shear zones, and only partially, if at all, modified the magnetic signature of the rocks.

Acknowledgements

We want to thank Rodney Allen, the journal editor William Dunne and the journal reviewers Jean Bouchez and Graham Borradaile for valuable comments on the manuscript, and Mai-Britt Mose Jensen for assistance in the AMS routines. This work is part of "VINNOVA 4D modelling of the Skellefte District" funded by VINNOVA, Boliden Mineral AB and Lundin Mining.

References

Allen, R.L., Weihed, P., Svenson, S.-Å, 1996. Setting of Zn–Cu–Au–Ag massive sulfide deposits in the evolution and facies architecture of a 1.9 Ga marine volcanic arc, Skellefte district, Sweden. Economic Geology 91, 1022–1053.

Årebäck, H., Barrett, T.J., Abrahamsson, S., Fagerström, P., 2005. The Palaeoproterozoic Kristineberg VMS deposit, Skellefte district, northern Sweden, part I: geology. Mineralium Deposita 40, 351–367.

Bauer, T., Skyttä, P., Weihed, P., Allen, R., 2009. 3D-modelling of the Central Skellefte District, Sweden. In: Proceedings of the 10th Biennial SGA Meeting, Townsville, Australia, 394–396.

Benn, K., Rochette, P., Bouchez, J.L., Hattori, K., 1993. Magnetic susceptibility, magnetic mineralogy, and magnetic fabrics in a late Archean granitoid-gneiss belt. Precambrian Research 63, 59–81.

Bergman Weihed, J., 2001. Palaeoproterozoic deformation zones in the Skellefte and the Arvidsjaur areas, northern Sweden. In: Weihed, P. (Ed.), Economic Geology Research 1. Sveriges Geologiska Undersökning C 833, pp. 46–68.

Bergström, U., Billström, K., Sträng, T., 1999. Age of the Viterliden intrusion, western Skellefte district, northern Sweden. In: Bergman, S. (Ed.), Radiometric Dating Results 4. Sveriges Geologiska Undersökning C 831, pp. 7–19.

Billström, K., Weihed, P., 1996. Age and provenance of host rocks and ores of the Palaeoproterozoic Skellefte District, northern Sweden. Economic Geology 91, 1054–1072.

Borradaile, G.J., 1988. Magnetic susceptibility, petrofabrics and strain. Tectonophysics 156, 1–20.

Borradaile, G.J., 1991. Correlation of strain with anisotropy of magnetic susceptibility (AMS). Pure and Applied Geophysics 135, 15–29.

Borradaile, G.J., Tarling, D., 1981. The influence of deformation mechanisms on magnetic fabrics in weakly deformed rocks. Tectonophysics 77, 151–168.

Borradaile, G.J., Henry, B., 1997. Tectonic applications of magnetic susceptibility and its anisotropy. Earth-Science Reviews 42, 49–93.

Borradaile, G.J., Puumala, M., Stupavsky, M., 1992. Anistotropy of complex magnetic susceptibility as an indicator of strain and petrofabric in rocks bearing sulphides. Tectonophysics 202, 309–318.

Bouchez, J.L., Gleizes, G., Djouadi, T., Rochette, P., 1990. Microstructure and magnetic susceptibility applied to emplacement kinematics of granites: the example of the Foix pluton (French Pyrenees). Tectonophysics 184, 157–171.

Bouchez, J.L., 1997. Granite is never isotropic: an introduction to AMS studies of granitic rocks. In: Bouchez, J.L., Hutton, D.H.W., Stephens, W.E. (Eds.), Granite: From Segregation of Melt to Emplacement Fabrics. Kluwer Academic Publishing, Rotterdam, pp. 95–112.

Elming, S.-Å., Mattsson, H.J., 2001. Post Jotnian basic intrusions in the Fennoscandian Shield, and the break up of Baltica from Laurentia: a paleomagnetic and AMS study. Precambrian Research 108, 215–236.

Evans, M.A., Lewchuk, M.T., Elmore, R.D., 2003. Strain partitioning of deformation mechanisms in limestones: examining the relationship of strain and anisotropy of magnetic susceptibility (AMS). Journal of Structural Geology 25, 1525–1549.

Galley, A.G., Bailes, A.H., 1999. The Interrelationship Between the Viterliden Intrusion, Synvolcanic Alteration, and Volcanogenic Massive Sulphide Mineralization, Kristineberg Region, Skellefte District, Sweden. CAMIRO, Project 94E07, Draft technical report (unpublished), 71 pp.

Goldstein, A.G., 1980. Magnetic susceptibility anisotropy of mylonites from the lake Char mylonite zone, southeastern New England. Tectonophysics 66, 197–211.

Hrouda, F., 1982. Magnetic anisotropy of rocks and its application in geology and geophysics. Geophysical Surveys 5, 37–82.

Hrouda, F., Janák, F., 1976. The changes in shape of the magnetic susceptibility ellipsoid during progressive metamorphism and deformation. Tectonophysics 34, 135–148.

Hrouda, F., Kahan, S., 1991. The magnetic fabric relationship between sedimentary and basement nappes in the High Tatra Mountains, N. Slovakia. Journal of Structural Geology 13, 431–442.

Hrouda, F., Jelinek, V., Zapletal, K., 1997. Refined technique for susceptibility resolution into ferromagnetic and paramagnetic components based on susceptibility temperature variation measurement. Geophysical Journal International 129, 715–719.

Jelinek, V., 1978. Statistical processing of anisotropy of magnetic susceptibility measured on groups of specimens. Studia Geophysica et Geodetica 22, 50–62.

Jelinek, V., 1981. Characterisation of the magnetic fabric of rocks. Tectonophysics 79, 63–67.

Kathol, B., Weihed, P. (Eds.), 2005. Description of Regional Geological and Geophysical Maps of the Skellefte District and Surrounding Areas. Sveriges Geologiska Undersökning Ba 57, p. 197.

Khan, M.A., 1962. The anisotropy of magnetic susceptibility of some igneous and metamorphic rocks. Journal of Geophysical Research 67, 2873–2885.

Kligfield, R., Lowrie, W., Dalziel, I.W.D., 1977. Magnetic susceptibility anisotropy as a strain indicator in the Sudbury basin, Ontario. Tectonophysics 40, 287–308.

Malehmir, A., Tryggvason, A., Lickorish, H., Weihed, P., 2007. Regional structural profiles in the western part of the Palaeoproterozoic Skellefte ore district, northern Sweden. Precambrian Research 159, 1–18.

Mattson, H.J., Elming, S.-Å, 2001. Magnetic fabrics and paleomagnetism of the Storsjön-Edsbyn deformation zone, central Sweden. Precambrian Research 107, 265–281.

Pares, J.M., van der Pluijm, B.A., 2002. Evaluating magnetic lineations (AMS) in deformed rocks. Tectonophysics 350, 283–298.

Pares, J.M., van der Pluijm, B.A., 2003. Magnetic fabrics and strain in pencil structures of the Knobs Formation, Valley and Ridge Province, US Appalachians. Journal of Structural Geology 25, 1349–1358.

Rathore, J.S., 1980. The magnetic fabrics of some slates from the Borrowdale volcanic group in the English Lake District and their correlations with strains. Tectonophysics 67, 207–220.

Rochette, P., Jackson, M., Aubourg, C., 1992. Rock magnetism and the interpretation of anisotropy of magnetic susceptibility. Reviews of Geophysics 30, 209–226.

Ruf, A.S., Naruk, S.J., Butler, R.F., Calderone, G.J., 1988. Strain and magnetic fabric in the Santa Catalina and Pinaleno Mountains metamorphic core complex mylonite zones, Arizona. Tectonics 7, 235–248.

Sagnotti, L., Speranza, S., 1993. Magnetic fabric analysis of the Plio–Pleistocene clayey units of the Sant'Arcangelo basin, southern Italy. Physics of the Earth and Planetary Interiors 77, 165–176.

Skyttä, P., Hermansson, T., Bauer, T., 2009. Three Dimensional Structure of the VMS-hosting Palaeoproterozoic Kristineberg Area, Northern Sweden. In: Proceedings of the 10th Biennial SGA Meeting, Townsville, Australia, 909–911.

Weihed, P., Bergman, J., Bergström, U., 1992. Metallogeny and tectonic evolution of the early Proterozoic Skellefte District, northern Sweden. Precambrian Research 58, 143–167.

Weihed, P., Billström, K., Persson, P.-O., Bergman Weihed, J., 2002. Relationship between 1.90–1.85 Ga accretionary processes and 1.82–1.80 Ga oblique subduction at the Karelian craton margin, Fennoscandian Shield. GFF 124, 163–180.